

On time-dependent analyses at $D\bar{D}$ threshold

Abstract

CP violation in the charm sector is a possible signature of new physics. Here we discuss the possibility to perform time-dependent analyses at $D\bar{D}$ threshold for CP violation searches.

Contents

1	Introduction	3
2	Mixing and CP, T and CPT violation in the neutral D system	4
2.1	Comparison of time-dependent measurements at $\Upsilon(4S)$ and at charm threshold	5
2.2	Comparison of time-dependent and time-integrated measurements at charm threshold	5
3	Sensitivities studies and main results	7
A	Time dependence of correlated decays with CP violation	15
A.1	Semileptonic decays with CP tag	15
A.2	Double $K^\mp\pi^\pm$ decays	16
A.3	Double semileptonic decays	17
A.4	$K^\mp\pi^\pm$ decays with CP tag	18
A.5	Double CP tag	19
A.6	Time-dependent Dalitz plot decay rates with CP violation	20
B	D^0-\bar{D}^0 mixing and CP violation with Dalitz plot analyses	24
B.1	Considerations for 3-body self-conjugate D^0 decay modes	24
B.2	Relevance of D^0 - \bar{D}^0 threshold data	25

1 Introduction

In this note we discuss the possibility to perform time-dependent measurements at $D\bar{D}$ threshold. This study has been triggered by the opportunity of having *relatively large* center-of-mass boost at $D\bar{D}$ threshold, possibly up to $\beta\gamma \simeq 0.9$, and we will try to address the issue if it is worth it or not for having such a large boost. We will base our advice on sensitivity estimates for CP violation (CPV) searches in the $D^0\bar{D}^0$ system and make a comparison with previous estimates reported in “SuperB Progress Reports – Physics” (2010) [1], where this possibility for time-dependent CPV ($TDCPV$) measurements at $D\bar{D}$ threshold was not considered. In the following, we assume an integrated luminosity of 500 fb^{-1} accumulated at the $\Psi(3770)$ (or $D\bar{D}$ threshold) with $\text{BR}(\Psi(3770) \rightarrow D^0\bar{D}^0) = (52 \pm 5) \times 10^{-2}$.

First of all, we should note an important difference between the neutral B and D meson systems related to the flavor tagging. The flavor tagging consist in determining the flavor of a neutral meson, M^0 , at time $t = 0$ and it represents a crucial information for time-dependent analyses. At B factories, the flavor of the D^0 is tagged at production ($t = 0$) through the decay $D^{*+} \rightarrow D^0\pi^+$, allowing for time-dependent measurements of D^0 originated in $e^+e^- \rightarrow c\bar{c}$ reactions (i.e. incoherent production). For the case of the neutral B mesons an analog method does not exist. The usage of a coherent production of neutral B mesons in the $\Upsilon(4S) \rightarrow B^0\bar{B}^0$ decay allows for time-dependent measurement of the other B of the event with respect to the B for which we tag the flavor. In this case, a center-of-mass boost is needed since the B mesons are produced almost at rest in the $\Upsilon(4S)$ rest frame. On the other hand, for the $D^0\bar{D}^0$ system, time-dependent measurements are possible at the $\Upsilon(4S)$ and the D^0 coherent production in the $\Psi(3770) \rightarrow D^0\bar{D}^0$ decay in principle is not necessary.

For this reason, in the following we will focus our attention on the peculiarities of $D\bar{D}$ threshold environment. In particular, the possibility to perform almost zero background measurements and the usage of CP -tagged D^0 events for time-dependent analyses, with the intent to identify golden modes for $TDCPV$ sensitivity studies.

The capability of CP tagging is a unique feature of $D\bar{D}$ threshold: by reconstructing one D of the event in a CP eigenstate the other D is determined to be in the opposite CP eigenstate. This technique has successfully exploited by CLEOc [3], which provided crucial information for a model-independent measurement of the CKM angle γ by Belle [2].

2 Mixing and CP , T and CPT violation in the neutral D system

In the following we use the PDG convention[4] to express the time-dependent decay amplitudes and rates of a neutral pseudoscalar meson $|M^0\rangle$ and its CP conjugate $|\bar{M}^0\rangle$.

$$|M_{\text{phys}}^0(t)\rangle = (g_+(t) + zg_-(t)) |M^0\rangle - \sqrt{1-z^2} \frac{q}{p} g_-(t) |\bar{M}^0\rangle \quad (1)$$

$$|\bar{M}_{\text{phys}}^0(t)\rangle = (g_+(t) - zg_-(t)) |\bar{M}^0\rangle - \sqrt{1-z^2} \frac{p}{q} g_-(t) |M^0\rangle \quad (2)$$

where

$$g_{\pm} = \frac{1}{2} \left(e^{-im_H t - \frac{1}{2}\Gamma_H t} \pm e^{-im_L t - \frac{1}{2}\Gamma_L t} \right) \quad (3)$$

and q, p are the parameters regulating indirect CP violation and z regulates CPT violation.

Defining $x \equiv \Delta m/\Gamma$ and $y \equiv \Delta\Gamma/(2\Gamma)$, and assuming $z = 0$, one obtains the following time-dependent decay rates:

$$\begin{aligned} \frac{d\Gamma[M_{\text{phys}}^0(t) \rightarrow f]/dt}{e^{-\Gamma t} \mathcal{N}_f} = & \\ & (|A_f|^2 + |(q/p)\bar{A}_f|^2) \cosh(y\Gamma t) + (|A_f|^2 - |(q/p)\bar{A}_f|^2) \cos(x\Gamma t) \\ & + 2\mathcal{R}e((q/p)A_f^* \bar{A}_f) \sinh(y\Gamma t) - 2\mathcal{I}m((q/p)A_f^* \bar{A}_f) \sin(x\Gamma t) \end{aligned} \quad (4)$$

$$\begin{aligned} \frac{d\Gamma[\bar{M}_{\text{phys}}^0(t) \rightarrow f]/dt}{e^{-\Gamma t} \mathcal{N}_f} = & \\ & (|(p/q)A_f|^2 + |\bar{A}_f|^2) \cosh(y\Gamma t) - (|(p/q)A_f|^2 - |\bar{A}_f|^2) \cos(x\Gamma t) \\ & + 2\mathcal{R}e((p/q)A_f \bar{A}_f^*) \sinh(y\Gamma t) - 2\mathcal{I}m((p/q)A_f \bar{A}_f^*) \sin(x\Gamma t) \end{aligned} \quad (5)$$

When neutral pseudoscalar mesons are produced coherently in pairs from the decay of a vector resonance, $V \rightarrow M^0 \bar{M}^0$, the time-dependence of their subsequent decays to final state f_1 and f_2 has a similar form to eqs. (4, 5):

$$\begin{aligned} \frac{d\Gamma[V_{\text{phys}}(t_1, t_2) \rightarrow f_1 f_2]/d\Delta t}{e^{-\Gamma|\Delta t|} \mathcal{N}_{f_1 f_2}} = & \\ & (|a_+|^2 + |a_-|^2) \cosh(y\Gamma \Delta t) + (|a_+|^2 - |a_-|^2) \cos(x\Gamma \Delta t) \\ & - 2\mathcal{R}e((a_+^* a_-) \sinh(y\Gamma \Delta t) + 2\mathcal{I}m(a_+^* a_-) \sin(x\Gamma \Delta t) \end{aligned} \quad (6)$$

where $\Delta t \equiv t_2 - t_1$ is the difference in the production times, t_1 and t_2 , of f_1 and f_2 , respectively, and the dependence on the average decay time and on decay angles has been integrated out. The coefficients a_+ and a_- are defined as

$$\begin{aligned} a_+ &\equiv \bar{A}_{f_1} A_{f_2} - A_{f_1} \bar{A}_{f_2}, \\ a_- &\equiv -\sqrt{1-z^2} \left(\frac{q}{p} \bar{A}_{f_1} \bar{A}_{f_2} - \frac{p}{q} A_{f_1} A_{f_2} \right) + z (\bar{A}_{f_1} A_{f_2} + A_{f_1} \bar{A}_{f_2}) \end{aligned} \quad (7)$$

2.1 Comparison of time-dependent measurements at $\Upsilon(4S)$ and at charm threshold

Time-dependent measurements performed at $\Upsilon(4S)$ use flavor-tagged D decays whose flavor at $t = 0$ is determined through the charge of the soft pion in the decay sequence $D^{*+} \rightarrow D^0\pi^+$ or $D^{*-} \rightarrow \bar{D}^0\pi^-$. The time-dependent rates are given in Eq. 4 and 5.

The same time-dependent rates can be measured also in $\Psi(3770) \rightarrow D\bar{D}$ decays if one of the D mesons is selected in a semi-leptonic final state. In fact, assuming CPT conservation ($z = 0$) and identifying $\Delta t \rightarrow t$ and $f_2 \rightarrow f$, we find that Eqs. 6 and 7 reduce to Eq. 4 if $A_{f_1} = 0$ and $\bar{A}_{f_1} = 1$, or to Eq. 5 if $\bar{A}_{f_1} = 0$ and $A_{f_1} = 1$.

At the charm threshold, however, the quantum coherence of the $D\bar{D}$ system gives access to a number of additional tag states other than the flavor-eigenstates D^0 or \bar{D}^0 . The relations between the time-dependent rate and the mixing/ $CP(T)$ parameters depend on the final state of the two D mesons in a way described by Eq. 6 and 7. In appendix A we have written explicitly these relations for several combinations of D final states. The list is also reported in Tab. ??.

2.2 Comparison of time-dependent and time-integrated measurements at charm threshold

Before analyzing the specific D final states at charm threshold it is instructive to make some general considerations regarding the comparison between the time-dependent and time-integrated measurements.

Since the mixing parameters x, y are small ($< 10^{-2}$) the time-dependent rate in Eq. 6 can be expanded by safely neglecting the terms $o(x^2), o(y^2)$:

$$\begin{aligned} \frac{d\Gamma[V_{\text{phys}}(t_1, t_2) \rightarrow f_1 f_2]/dt}{e^{-\Gamma|\Delta t|}\mathcal{N}_{f_1 f_2}} = \\ 2|a_+|^2 + \left(\frac{y^2 - x^2}{2}|a_+|^2 + \frac{y^2 + x^2}{2}|a_-|^2 \right) (\Gamma\Delta t)^2 + \\ 2(-y\mathcal{R}e(a_+^* a_-) + x\mathcal{I}m(a_+^* a_-)) \Gamma\Delta t \end{aligned} \quad (8)$$

Analogously, after neglecting terms of order $o(x^2)$ and $o(y^2)$ the time-integrated rate can be written as:

$$\Gamma = \int \frac{d\Gamma}{d\Delta t} d\Delta t \propto \frac{2}{\Gamma} ((2 + y^2 - x^2)|a_+|^2 + (y^2 + x^2)|a_-|^2) \quad (9)$$

Let us compare Eq. 8 and 9. Both the time-dependent and time-independent measurements are usually mostly sensitive to the term $|a_+|^2$, except for specific cases as for example the double semileptonic tag where $a_+ = 0$ (see appendix A). The term $|a_-|^2$ is in both cases suppressed by $x^2 + y^2 \sim 10^{-4} - 10^{-5}$. The time-dependent rate keeps in addition the dependence on $-y\mathcal{R}e(a_+^* a_-) + x\mathcal{I}m(a_+^* a_-)$. This term constitutes the substantial difference between the time-dependent and the time-integrated measurements.

Our next steps can be summarized as follows

- evaluate what additional information is provided by the quantity $-y\mathcal{R}e(a_+^*a_-) + x\mathcal{I}m(a_+^*a_-)$, as a function of the selected D final states
- study how the sensitivity on the physics parameters extracted from $-y\mathcal{R}e(a_+^*a_-) + x\mathcal{I}m(a_+^*a_-)$, $|a_+|^2$ and $|a_-|^2$ scale as a function of the CM boost

Regarding the second item there are two competing factors that must be evaluated. One is how the time resolution improves as the boost increases, and how the improved time resolution affects the precision of the physics parameters extracted from the time-dependent measurement. The other factor is how the reconstruction efficiency reduces as the boost increases, and consequently what is the effect on the precision of the physics parameters.

At this time we have performed preliminary studies based on the selection of double $K^\pm\pi^\mp$ decays to quantify how the time resolution and the reconstruction efficiency scale as a function of the boost. The results are summarized in Fig. 1 and 2. We still have to evaluate how the error of the physics parameters extracted from the time-dependent measurement is affected by the time resolution.

3 Sensitivities studies and main results

average Δt error vs boost

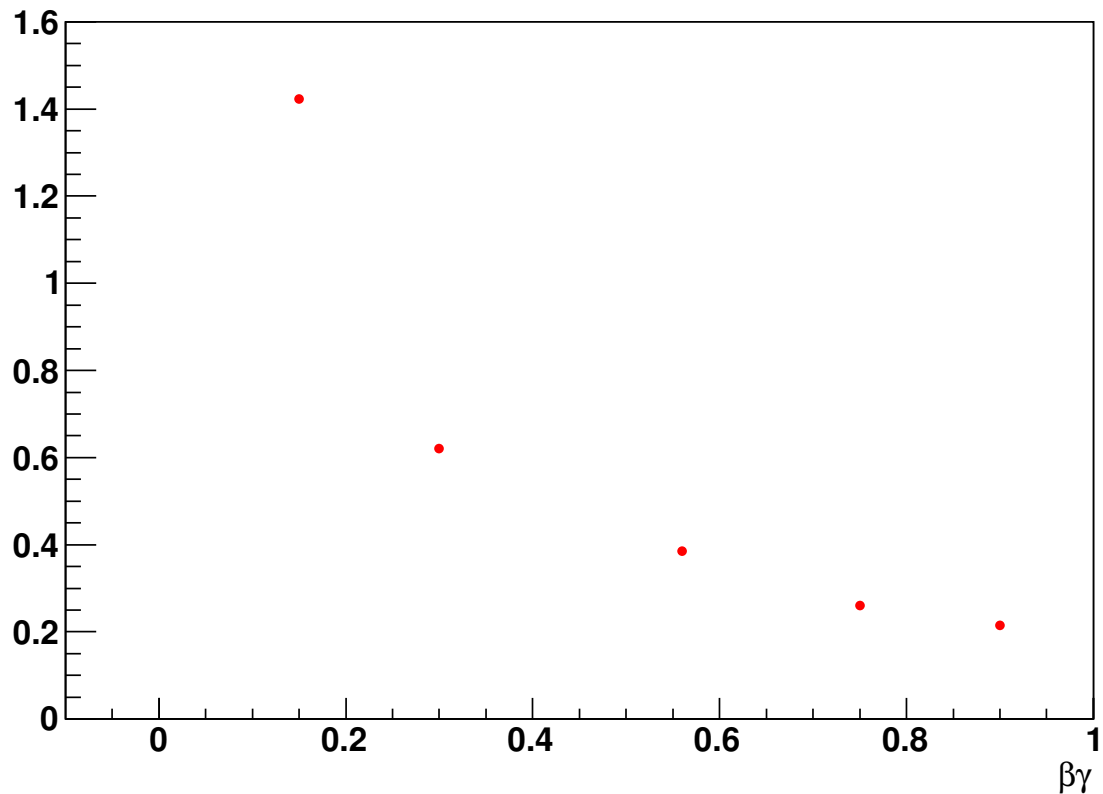


Figure 1: Average error [ps] of the reconstructed proper time difference between the two D mesons in the decay $\Psi(3770) \rightarrow D\bar{D}$ with $D \rightarrow K^-\pi^+$, $\bar{D} \rightarrow K^-\pi^+$, as a function of the CM boost. As a comparison, the D^0 lifetime is 0.4 ps.

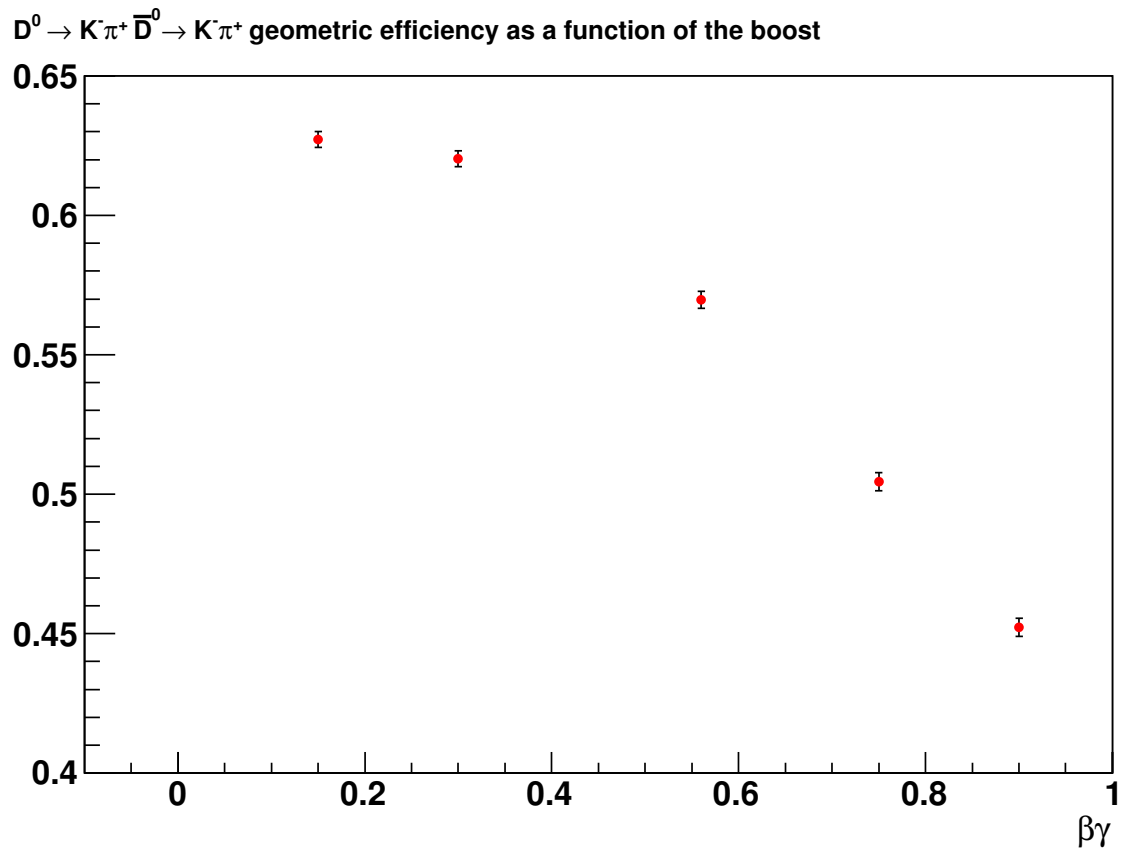


Figure 2: Reconstruction efficiency of the decay $\Psi(3770) \rightarrow D\bar{D}$ with $D \rightarrow K^- \pi^+$, $\bar{D} \rightarrow K^- \pi^+$ as a function of the CM boost. The signal candidates are truth-matched and no additional selection cuts are applied, therefore the efficiency is essentially geometric.

Selected decays	$\Upsilon(4S)$ 75 ab ⁻¹	$\Psi(3770)$ 0.5 ab ⁻¹ , $\beta\gamma = 0.238$	$\Psi(3770)$ 0.5 ab ⁻¹ , $\beta\gamma = 0.56$	$\Psi(3770)$ 0.5 ab ⁻¹ , $\beta\gamma = 0.91$
$l^\pm X^\mp, CP+$	19600000	569395	525890	418331
$l^\pm X^\mp, CP-$	30900000	685053	612430	491599
$l^\pm X^\mp, K^\pm\pi^\mp$	222900000 (790000)	4181494 (13798)	3862011 (12744)	3072118 (10137)
$l^\pm X^\mp, K_S^0\pi^+\pi^-$	86600000	828850	689557	498370
$l^\pm X^\mp, l^\mp X^\pm$	85300000 (50)	1067615 (51)	986045 (47)	784370 (38)
$K^\mp\pi^\pm, K^\pm\pi^\mp$	N/A (N/A)	1067615 (51)	986045 (47)	784370 (38)
$CP+, K^\mp\pi^\pm$	N/A	309608	285953	227467
$CP-, K^\mp\pi^\pm$	N/A	291814	260879	209408
$CP+, CP-$	N/A	92526	82717	66397
$CP+, K_S^0\pi^+\pi^-$	N/A	113691	91553	66770
$CP-, K_S^0\pi^+\pi^-$	N/A	115525	93030	67847
$K_S^0\pi^+\pi^-, K_S^0\pi^+\pi^-$	N/A	290342	217578	142875

Table 1: Expected number of events as a function of the reconstructed decays. For the run at $\Psi(3770)$ we assume an integrated luminosity of 0.5 ab⁻¹ and we consider 3 scenarios for the CM boost, from 0.238 up to 0.91. The label “ $l^\pm X^\mp$ ” for the $\Upsilon(4S)$ run should be read as “at $t = 0$ the D flavor was determined to be D^0 ($l^+ X^-$) or \bar{D}^0 ($l^- X^+$) through the selection of the $D^{*\pm} \rightarrow D^0/\bar{D}^0\pi^\pm$ decay”. All numbers are preliminary. N/A=Not Available. Numbers in parenthesis correspond to the suppressed decays, assuming current WA values for mixing and DCS to CF ratio.

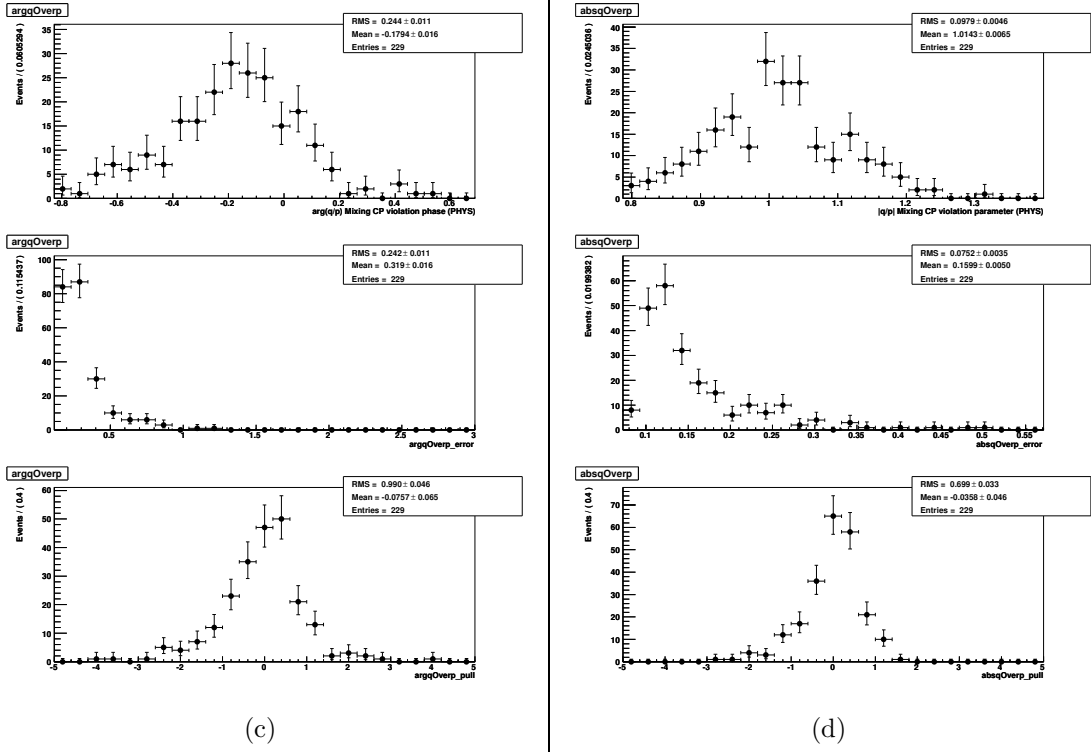
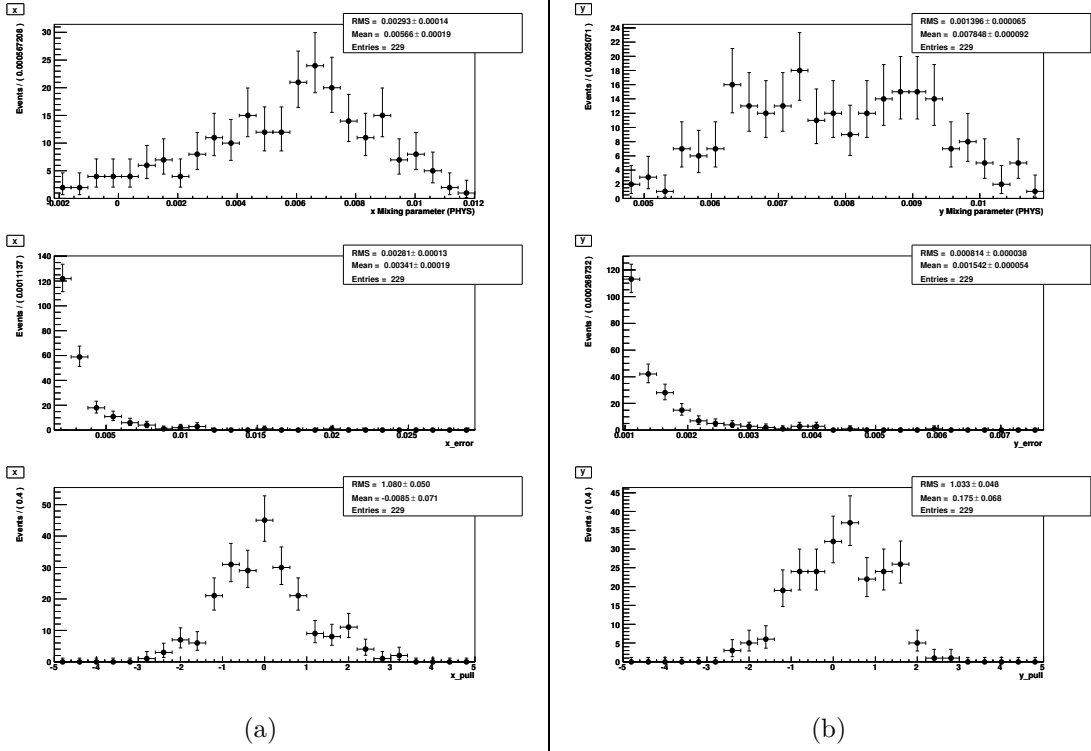


Figure 3: Central values, errors and pulls for the mixing and CP-violating parameters from the fit to the $\Psi(3770)$ Monte Carlo experiments, with perfect resolution and no mistag. The statistics for each of the 8 two-body double-tags is 1/10 of what is reported in the 3rd column of Table 1. The generated values are the current HFAG values, $x = 0.00628$, $y = 0.00747$, $|q/p| = 1$, $\phi = -0.179$ rad, $\delta_{K\pi} = 3.525$ rad.

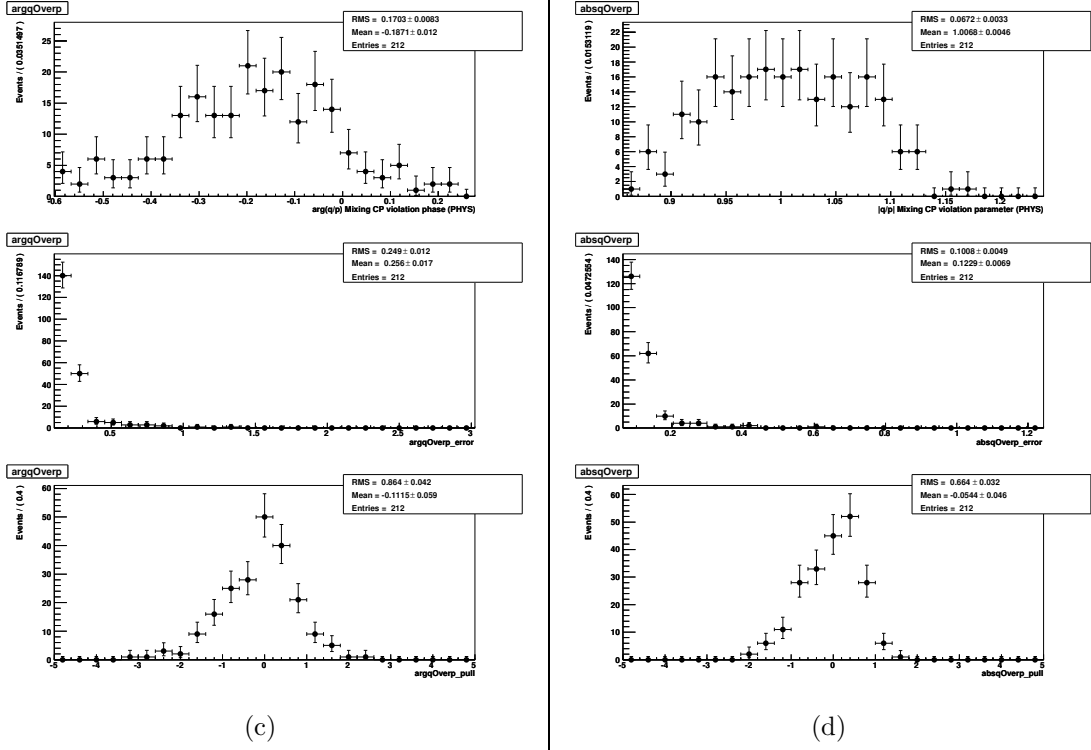
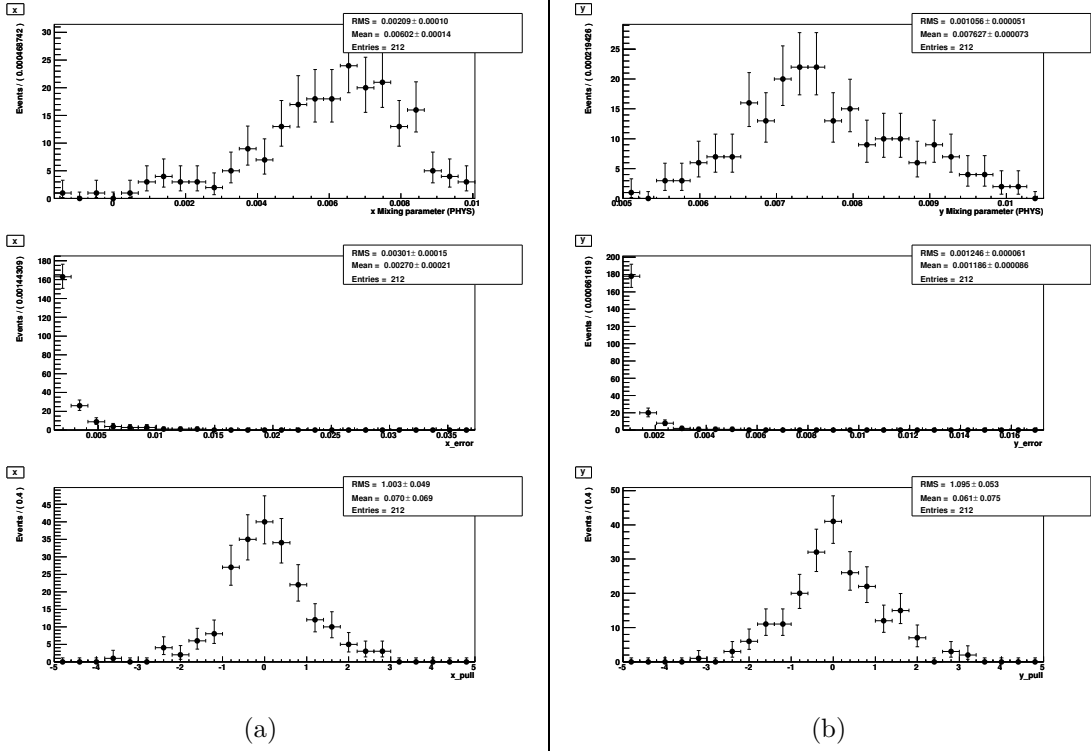


Figure 4: Central values, errors and pulls for the mixing and CP-violating parameters from the fit to the $\Upsilon(4S)$ Monte Carlo experiments, with perfect resolution and no mistag. The statistics for each of the 4 two-body double-tags is 1/200 of what is reported in the 2nd column of Table 1. The generated values are the current HFAG values, $x = 0.00628$, $y = 0.00747$, $|q/p| = 1$, $\phi = -0.179$ rad, $\delta_{K\pi} = 3.525$ rad.

Data	Time resolution	Mistag	$\sigma(x)$	$\sigma(y)$	$\sigma(\phi)$	$\sigma(q/p)$
LB $\Psi(3770)$	Perfect	0	0.00293	0.00140	0.244	0.0979
LB $\Psi(3770)$ large mixing	Perfect	0	0.00188	0.00137	0.023	0.0085
LB $\Psi(3770)$ no CPV	Perfect	0	0.00256	0.00086	0	0
LB $\Psi(3770)$	HB TG (0.25/0.20 ps)	0	0.00309	0.00146	0.243	0.1067
LB $\Psi(3770)$	IB TG (0.40/0.28 ps)	0	0.00316	0.00160	0.248	0.1093
LB $\Psi(3770)$	LB TG (0.66/0.39 ps)	0	0.00330	0.00171	0.327	0.1164
LB $\Psi(3770)$	VLB TG (1.27/0.76 ps)	0	0.00337	0.00212	0.472	0.192
HB $\Psi(3770)$	HB TG (0.25/0.20 ps)	0	0.00374	0.00177	0.294	0.129
IB $\Psi(3770)$	IB TG (0.40/0.28 ps)	0	0.00340	0.00172	0.267	0.118
LB $\Psi(3770)$	Perfect	2%	0.00663	0.00196	0.377	0.308
$\Upsilon(4S)$	Perfect	0	0.00290	0.00106	0.170	0.0672
$\Upsilon(4S)$ large mixing	Perfect	0	0.00141	0.00112	0.016	0.0065
$\Upsilon(4S)$ no CPV	Perfect	0	0.00174	0.00058	0	0
$\Upsilon(4S)$	TG (0.17/0.10 ps)	0	0.00234	0.00113	0.197	0.0702
$\Upsilon(4S)$	Perfect	2%	0.00418	0.00156	0.270	0.192

Table 2: Estimated sensitivities for the mixing and CP violating parameters as determined from combined fits to all two-body double tags available at $\Psi(3770)$ and Υ , using the expected number of events and proper time resolution as a function of the reconstructed decays from Table 1. “LB $\Psi(3770)$ ”, “IB $\Psi(3770)$ ” and “HB $\Psi(3770)$ ” data refer to the low ($\beta\gamma = 0.238$), intermediate ($\beta\gamma = 0.56$) and high ($\beta\gamma = 0.91$) boost number of events, given in the 3rd, 4th and 5th columns, respectively, in Table 1. According to Figure 2, the expected number of events is approximately stable for $\beta\gamma$ in the range between 0.15 and 0.3. “HB TG”, “IB TG”, “LB TG” and “VLB TG” refer to the high ($\beta\gamma = 0.91$), intermediate ($\beta\gamma = 0.56$), low ($\beta\gamma = 0.3$) and very low ($\beta\gamma = 0.15$) triple Gaussian proper time resolution at $\Psi(3770)$ as estimated from FastSim and reported in Figure 1. The numbers in parenthesis are the total and core rms resolutions. The “large mixing” configuration has been generated with x and y values 10 times larger than the nominal (HFAG) values. The reported (rms) sensitivities for the mixing and CP violating parameters are for /10 and /200 the estimated number of events, for $\Psi(3770)$ and $\Upsilon(4S)$ data. The corresponding sensitivities to the complete expected SuperB data can be extracted scaling those values by $\sqrt{10}$ and $\sqrt{200}$.

Data	Time resolution	Mistag	$\sigma(x)$	$\sigma(y)$	$\sigma(\phi)$	$\sigma(q/p)$
LB $\Psi(3770)$	Perfect	0	0.00076	0.00044	0.077	0.031
LB $\Psi(3770)$ large mixing	Perfect	0	0.00059	0.00043	0.007	0.003
LB $\Psi(3770)$ no CPV	Perfect	0	0.00081	0.00027	0	0
LB $\Psi(3770)$	HB TG (0.25/0.20 ps)	0	0.00098	0.00046	0.077	0.034
LB $\Psi(3770)$	IB TG (0.40/0.28 ps)	0	0.00100	0.00051	0.078	0.035
LB $\Psi(3770)$	LB TG (0.66/0.39 ps)	0	0.00104	0.00054	0.103	0.037
LB $\Psi(3770)$	VLB TG (1.27/0.76 ps)	0	0.00107	0.00067	0.149	0.061
HB $\Psi(3770)$	HB TG (0.25/0.20 ps)	0	0.00118	0.00056	0.093	0.041
IB $\Psi(3770)$	IB TG (0.40/0.28 ps)	0	0.00108	0.00054	0.084	0.037
LB $\Psi(3770)$	Perfect	2%	0.00210	0.00062	0.119	0.097
$\Upsilon(4S)$	Perfect	0	0.00021	0.00007	0.012	0.005
$\Upsilon(4S)$ large mixing	Perfect	0	0.00010	0.00008	0.001	0.001
$\Upsilon(4S)$ no CPV	Perfect	0	0.00012	0.00004	0	0
$\Upsilon(4S)$	TG (0.17/0.10 ps)	0	0.00017	0.00008	0.014	0.005
$\Upsilon(4S)$	Perfect	2%	0.00030	0.00011	0.019	0.014

Table 3: Estimated sensitivities for the mixing and CP violating parameters as determined from combined fits to all two-body double tags available at $\Psi(3770)$ and Υ , using the expected number of events and proper time resolution as a function of the reconstructed decays from Table 1. “LB $\Psi(3770)$ ”, “IB $\Psi(3770)$ ” and “HB $\Psi(3770)$ ” data refer to the low ($\beta\gamma = 0.238$), intermediate ($\beta\gamma = 0.56$) and high ($\beta\gamma = 0.91$) boost number of events, given in the 3rd, 4th and 5th columns, respectively, in Table 1. According to Figure 2, the expected number of events is approximately stable for $\beta\gamma$ in the range between 0.15 and 0.3. “HB TG”, “IB TG”, “LB TG” and “VLB TG” refer to the high ($\beta\gamma = 0.91$), intermediate ($\beta\gamma = 0.56$), low ($\beta\gamma = 0.3$) and very low ($\beta\gamma = 0.15$) triple Gaussian proper time resolution at $\Psi(3770)$ as estimated from FastSim and reported in Figure 1. The numbers in parenthesis are the total and core rms resolutions. The “large mixing” configuration has been generated with x and y values 10 times larger than the nominal (HFAG) values. The reported (rms) sensitivities for the mixing and CP violating parameters have been scaled to the complete expected SuperB data by scaling by $\sqrt{10}$ and $\sqrt{200}$ the rms results from the Toy Monte Carlo experiments.

References

- [1] B. O’Leary *et al.* [SuperB Collaboration], “SuperB Progress Reports – Physics,” [arXiv:1008.1541 [hep-ex]].
- [2] A. Poluektov [Belle Collaboration], “First measurement of $\gamma(\phi_3)$ with model-independent Dalitz plot,” Presentation at Moriond EW (2011) <http://belle.kek.jp/belle/talks/moriondEW11/poluektov.pdf>
- [3] R. A. Briere *et al.* [CLEO Collaboration], “First model-independent determination of the relative strong phase between D^0 and $\bar{D}^0 \rightarrow K_S^0 \pi^+ \pi^-$ and its impact on the CKM angle $\gamma/\phi(3)$ measurement,” Phys. Rev. **D80**, 032002 (2009). [arXiv:0903.1681 [hep-ex]].
- [4] *CP violation review in the Review of Particle Physics 2010*, K. Nakamura *et al.*, J. Phys. G **37**, 075021 (2010).
- [5] D. M. Asner *et al.* [CLEO Collaboration], “Search for $D^0 - \bar{D}^0$ mixing in the Dalitz plot analysis of $D^0 \rightarrow K_S^0 \pi^+ \pi^-$,” Phys. Rev. D **72**, 012001 (2005) [arXiv:hep-ex/0503045].
- [6] P. del Amo Sanchez *et al.* [The BABAR Collaboration], “Measurement of D^0 -anti D^0 mixing parameters using $D^0 \rightarrow K_S^0 \pi^+ \pi^-$ and $D^0 \rightarrow K_S^0 K^+ K^-$ decays,” Phys. Rev. Lett. **105**, 081803 (2010) [arXiv:1004.5053 [hep-ex]].
- [7] B. Aubert *et al.* [BABAR Collaboration], “Measurement of $D^0 - \bar{D}^0$ mixing from a time-dependent amplitude analysis of $D^0 \rightarrow K^+ \pi^- \pi^0$ decays,” Phys. Rev. Lett. **103**, 211801 (2009) [arXiv:0807.4544 [hep-ex]].
- [8] K. Abe *et al.* [BELLE Collaboration], “Measurement of $D^0 - \bar{D}^0$ mixing in $D^0 \rightarrow K_S^0 \pi^+ \pi^-$ decays,” Phys. Rev. Lett. **99**, 131803 (2007) [arXiv:0704.1000 [hep-ex]].
- [9] A. Bondar, A. Poluektov, “The Use of quantum-correlated D^0 decays for ϕ_3 measurement,” Eur. Phys. J. **C55**, 51-56 (2008). [arXiv:0801.0840 [hep-ex]].
- [10] A. Bondar, A. Poluektov, V. Vorobiev, “Charm mixing in the model-independent analysis of correlated $D^0 \bar{D}^0$ decays,” Phys. Rev. **D82**, 034033 (2010). [arXiv:1004.2350 [hep-ph]].

A Time dependence of correlated decays with CP violation

Here we report the expressions for the time dependence of correlated decays at $D^0\bar{D}^0$ threshold accounting for possible indirect CP violation (i.e. $|q/p| \neq 1$, $\phi \neq 0$). For the sake of simplicity we assume CPT is conserved and also CP is conserved in the decay and reserve the possibility of considering CP violation in the decay and CPT violation for more general sensitivity studies. The phase convention that we use is:

$$CP|D^0\rangle = |\bar{D}^0\rangle \quad (10)$$

so that:

$$\lambda_{f_{CP}} = \frac{q}{p} \frac{\bar{A}_{f_{CP}}}{A_{f_{CP}}} = \eta \left| \frac{q}{p} \right| e^{i\phi} \quad (11)$$

The final states that we consider are:

1. S_η , a CP eigenstate of eigenvalue $\eta = \pm 1$;
2. a flavor specific semi-leptonic decays to a final state containing $l^\pm X^\mp$ is an inclusive set of all final states;
3. G , hadronic final state such that both D^0 and \bar{D}^0 can decay to it. For example, in charmed mesons, $D^0 \rightarrow G^+$ is Cabibbo Favored (CF) and $D^0 \rightarrow G^-$ is doubly Cabibbo suppressed, as in $D^0 \rightarrow K^-\pi^+$. This implies that the ratio of DCS to CA decay rates R is small and the results can be expanded in terms of this ratio.

The time-dependent decay rates $R_{odd}(f_1, f_2, \Delta t)$ for antisymmetric initial state ($C=\text{odd}$) into final states f_1, f_2 are reported below and can be derived from Eq. 6 with the substitution

$$R_{odd}(f_1, f_2, \Delta t) = \frac{d\Gamma[V_{\text{phys}}(t_1, t_2) \rightarrow f_1 f_2]/dt}{e^{-\Gamma|\Delta t|} \mathcal{N}_{f_1 f_2}} \quad (12)$$

In the next sections we consider several combinations of final states (f_1, f_2) and we write explicitly the time-dependent and time-integrated rates.

A.1 Semileptonic decays with CP tag

$$\begin{aligned}
 R_{odd}(l^- X^+, S_\eta; \Delta t) &= |\bar{A}_{l^- X^+} A_{S_\eta}|^2 \left\{ \left(1 + \left| \frac{q}{p} \right|^2 \right) \cosh(y\Gamma\Delta t) + \left(1 - \left| \frac{q}{p} \right|^2 \right) \cos(x\Gamma\Delta t) \right. \\
 &\quad \left. + 2\eta \left| \frac{q}{p} \right| \cos\phi \sinh(y\Gamma\Delta t) - 2\eta \left| \frac{q}{p} \right| \sin\phi \sin(x\Gamma\Delta t) \right\} \\
 R_{odd}(l^+ X^-, S_\eta; \Delta t) &= |A_{l^+ X^-} A_{S_\eta}|^2 \left\{ \left(1 + \left| \frac{p}{q} \right|^2 \right) \cosh(y\Gamma\Delta t) + \left(1 - \left| \frac{p}{q} \right|^2 \right) \cos(x\Gamma\Delta t) \right. \\
 &\quad \left. + 2\eta \left| \frac{p}{q} \right| \cos\phi \sinh(y\Gamma\Delta t) + 2\eta \left| \frac{p}{q} \right| \sin\phi \sin(x\Gamma\Delta t) \right\}
 \end{aligned} \quad (13)$$

In the limit of $|x\Gamma\Delta t| \ll 1$, $|y\Gamma\Delta t| \ll 1$ we obtain:

$$\begin{aligned}
R_{odd}(l^- X^+, S_\eta; \Delta t) &= 2 |\bar{A}_{l^- X^+} A_{S_\eta}|^2 \left\{ \right. \\
&\quad \left. 1 + \eta \left| \frac{q}{p} \right| (y \cos \phi - x \sin \phi) (\Gamma \Delta t) + \left(\frac{y^2}{4} \left(1 + \left| \frac{q}{p} \right|^2 \right) - \frac{x^2}{4} \left(1 - \left| \frac{q}{p} \right|^2 \right) \right) (\Gamma \Delta t)^2 \right\} \\
R_{odd}(l^+ X^-, S_\eta; \Delta t) &= 2 |A_{l^+ X^-} A_{S_\eta}|^2 \left\{ \right. \\
&\quad \left. 1 + \eta \left| \frac{p}{q} \right| (y \cos \phi + x \sin \phi) (\Gamma \Delta t) + \left(\frac{y^2}{4} \left(1 + \left| \frac{p}{q} \right|^2 \right) - \frac{x^2}{4} \left(1 - \left| \frac{p}{q} \right|^2 \right) \right) (\Gamma \Delta t)^2 \right\}
\end{aligned} \tag{14}$$

identical time-dependent decay rate as for the case of $D^0 \rightarrow f_{CP}$ at $\Upsilon(4S)$.

Integrating 13 or 14 over time we obtain:

$$\begin{aligned}
\int R_{odd}(l^- X^+, S_\eta; \Delta t) e^{-\Gamma|\Delta t|} d(\Delta t) &= \\
&\quad \frac{4}{\Gamma} |\bar{A}_{l^- X^+} A_{S_\eta}|^2 \left[1 + \frac{y^2}{2} \left(1 + \left| \frac{q}{p} \right|^2 \right) - \frac{x^2}{2} \left(1 - \left| \frac{q}{p} \right|^2 \right) \right] \\
\int R_{odd}(l^+ X^-, S_\eta; \Delta t) e^{-\Gamma|\Delta t|} d(\Delta t) &= \\
&\quad \frac{4}{\Gamma} |A_{l^+ X^-} A_{S_\eta}|^2 \left[1 + \frac{y^2}{2} \left(1 + \left| \frac{p}{q} \right|^2 \right) - \frac{x^2}{2} \left(1 - \left| \frac{p}{q} \right|^2 \right) \right]
\end{aligned} \tag{15}$$

A.2 Double $K^\mp \pi^\pm$ decays

For the case of hadronic final state G , it is interesting to consider the time-dependent decay rate for the final state $(K^+ \pi^-, K^+ \pi^-)$ (and for charge conjugate). It is useful to introduce the following quantities and phase conventions:

$$\frac{\bar{A}_{K^-\pi^+}}{A_{K^-\pi^+}} \equiv \frac{A_{K^+\pi^-}}{\bar{A}_{K^+\pi^-}} = -\sqrt{R_D} e^{-i\delta_{K\pi}} \tag{16}$$

$$\lambda_{K^-\pi^+} = \frac{q \bar{A}_{K^-\pi^+}}{p A_{K^-\pi^+}} = -\left| \frac{q}{p} \right| \sqrt{R_D} e^{-i(\delta_{K\pi} - \phi)} \tag{17}$$

$$\bar{\lambda}_{K^+\pi^-} = \frac{p A_{K^+\pi^-}}{q \bar{A}_{K^+\pi^-}} = -\left| \frac{p}{q} \right| \sqrt{R_D} e^{-i(\delta_{K\pi} + \phi)} \tag{18}$$

$$\begin{aligned}
R_{odd}(K^-\pi^+, K^-\pi^+; \Delta t) &= |A_{K^-\pi^+}|^4 \left| \frac{p}{q} \right|^2 |1 - \lambda_{K^-\pi^+}^2|^2 [\cosh(y\Gamma\Delta t) - \cos(x\Gamma\Delta t)] \\
R_{odd}(K^+\pi^-, K^+\pi^-; \Delta t) &= |\bar{A}_{K^+\pi^-}|^4 \left| \frac{q}{p} \right|^2 |1 - \bar{\lambda}_{K^+\pi^-}^2|^2 [\cosh(y\Gamma\Delta t) - \cos(x\Gamma\Delta t)]
\end{aligned} \tag{19}$$

In the limit of $|x\Gamma\Delta t| \ll 1$, $|y\Gamma\Delta t| \ll 1$ we obtain:

$$\begin{aligned}
R_{odd}(K^-\pi^+, K^-\pi^+; \Delta t) &= |A_{K^-\pi^+}|^4 \left| \frac{p}{q} \right|^2 \left[1 + \left| \frac{q}{p} \right|^4 R_D^2 - 2R_D \left| \frac{q}{p} \right|^2 \cos[2(\delta_{K\pi} - \phi)] \right] \frac{x^2 + y^2}{2} (\Gamma\Delta t)^2 \\
R_{odd}(K^+\pi^-, K^+\pi^-; \Delta t) &= |A_{K^+\pi^-}|^4 \left| \frac{q}{p} \right|^2 \left[1 + \left| \frac{p}{q} \right|^4 R_D^2 - 2R_D \left| \frac{p}{q} \right|^2 \cos[2(\delta_{K\pi} + \phi)] \right] \frac{x^2 + y^2}{2} (\Gamma\Delta t)^2
\end{aligned} \tag{20}$$

Integrating 19 or 20 over time we obtain:

$$\begin{aligned}
\int R_{odd}(K^-\pi^+, K^-\pi^+; \Delta t) e^{-\Gamma|\Delta t|} d(\Delta t) &= \\
&\frac{2}{\Gamma} |A_{K^-\pi^+}|^4 \left| \frac{p}{q} \right|^2 \left[1 + \left| \frac{q}{p} \right|^4 R_D^2 - 2R_D \left| \frac{q}{p} \right|^2 \cos[2(\delta_{K\pi} - \phi)] \right] (x^2 + y^2) \\
\int R_{odd}(K^+\pi^-, K^+\pi^-; \Delta t) e^{-\Gamma|\Delta t|} d(\Delta t) &= \\
&\frac{2}{\Gamma} |A_{K^+\pi^-}|^4 \left| \frac{q}{p} \right|^2 \left[1 + \left| \frac{p}{q} \right|^4 R_D^2 - 2R_D \left| \frac{p}{q} \right|^2 \cos[2(\delta_{K\pi} + \phi)] \right] (x^2 + y^2)
\end{aligned} \tag{21}$$

A.3 Double semileptonic decays

For the case of double flavor specific final states ($l^+ X^-$, $l^+ X^-$) (and charge conjugate) we have:

$$\begin{aligned}
R_{odd}(l^+ X^-, l^+ X^-; \Delta t) &= |A_{l^+ X^-}|^4 \left| \frac{p}{q} \right|^2 [\cosh(y\Gamma\Delta t) - \cos(x\Gamma\Delta t)] \\
R_{odd}(l^- X^+, l^- X^+; \Delta t) &= |A_{l^- X^+}|^4 \left| \frac{q}{p} \right|^2 [\cosh(y\Gamma\Delta t) - \cos(x\Gamma\Delta t)]
\end{aligned} \tag{22}$$

In the limit of $|x\Gamma\Delta t| \ll 1$, $|y\Gamma\Delta t| \ll 1$ we obtain:

$$\begin{aligned}
R_{odd}(l^+ X^-, l^+ X^-; \Delta t) &= |A_{l^+ X^-}|^4 \left| \frac{p}{q} \right|^2 \frac{x^2 + y^2}{2} (\Gamma\Delta t)^2 \\
R_{odd}(l^- X^+, l^- X^+; \Delta t) &= |A_{l^- X^+}|^4 \left| \frac{q}{p} \right|^2 \frac{x^2 + y^2}{2} (\Gamma\Delta t)^2
\end{aligned} \tag{23}$$

Integrating 22 and 23 over time we obtain:

$$\begin{aligned}
\int R_{odd}(l^+ X^-, l^+ X^-; \Delta t) e^{-\Gamma|\Delta t|} d(\Delta t) &= \frac{2}{\Gamma} |A_{l^+ X^-}|^4 \left| \frac{p}{q} \right|^2 (x^2 + y^2) \\
\int R_{odd}(l^- X^+, l^- X^+; \Delta t) e^{-\Gamma|\Delta t|} d(\Delta t) &= \frac{2}{\Gamma} |A_{l^- X^+}|^4 \left| \frac{q}{p} \right|^2 (x^2 + y^2)
\end{aligned} \tag{24}$$

A.4 $K^\mp \pi^\pm$ decays with CP tag

For the case of CP tag we consider for example $(S_\eta, K^- \pi^+)$. We have:

$$\begin{aligned}
R_{odd}(S_\eta, K^- \pi^+; \Delta t) &= |A_{S_\eta} A_{K^- \pi^+}|^2 \left\{ \right. \\
&\left[\left(1 + \left| \frac{p}{q} \right|^2 \right) + 2\eta \sqrt{R_D} (\cos \delta_{K\pi} + \cos(\delta_{K\pi} - 2\phi)) + R_D \left(1 + \left| \frac{q}{p} \right|^2 \right) \right] \cosh(y\Gamma\Delta t) \\
&+ \left[\left(1 - \left| \frac{p}{q} \right|^2 \right) + 2\eta \sqrt{R_D} (\cos \delta_{K\pi} - \cos(\delta_{K\pi} - 2\phi)) + R_D \left(1 - \left| \frac{q}{p} \right|^2 \right) \right] \cos(x\Gamma\Delta t) \\
&- 2 \left[\eta \left| \frac{p}{q} \right| \cos \phi + \sqrt{R_D} \cos(\delta_{K\pi} - \phi) \left(\left| \frac{q}{p} \right| + \left| \frac{p}{q} \right| \right) + R_D \left| \frac{q}{p} \right| \cos \phi \right] \sinh(y\Gamma\Delta t) \\
&+ 2 \left[-\eta \left| \frac{p}{q} \right| \sin \phi + \sqrt{R_D} \sin(\delta_{K\pi} - \phi) \left(\left| \frac{q}{p} \right| - \left| \frac{p}{q} \right| \right) + R_D \left| \frac{q}{p} \right| \sin \phi \right] \sin(y\Gamma\Delta t) \left. \right\} \tag{25}
\end{aligned}$$

In the limit of $|x\Gamma\Delta t| \ll 1$, $|y\Gamma\Delta t| \ll 1$ we obtain:

$$\begin{aligned}
R_{odd}(S_\eta, K^- \pi^+; \Delta t) &= |A_{S_\eta} A_{K^- \pi^+}|^2 \left\{ 2 \left(1 + 2\eta \sqrt{R_D} \cos \delta_{K\pi} + R_D \right) \right. \\
&+ \left[\left(\eta \left| \frac{p}{q} \right| \cos \phi + \sqrt{R_D} \cos(\delta_{K\pi} - \phi) \left(\left| \frac{q}{p} \right| + \left| \frac{p}{q} \right| \right) + R_D \left| \frac{q}{p} \right| \cos \phi \right) y \right. \\
&+ \left. \left. \left(-\eta \left| \frac{p}{q} \right| \sin \phi + \sqrt{R_D} \sin(\delta_{K\pi} - \phi) \left(\left| \frac{q}{p} \right| - \left| \frac{p}{q} \right| \right) + R_D \left| \frac{q}{p} \right| \sin \phi \right) x \right] (\Gamma\Delta t) \right. \\
&+ \frac{1}{2} \left[\left(\left(1 + \left| \frac{p}{q} \right|^2 \right) + 2\eta \sqrt{R_D} (\cos \delta_{K\pi} + \cos(\delta_{K\pi} - 2\phi)) + R_D \left(1 + \left| \frac{q}{p} \right|^2 \right) \right) y^2 \right. \\
&- \left. \left. \left(\left(1 - \left| \frac{p}{q} \right|^2 \right) + 2\eta \sqrt{R_D} (\cos \delta_{K\pi} - \cos(\delta_{K\pi} - 2\phi)) + R_D \left(1 - \left| \frac{q}{p} \right|^2 \right) \right) x^2 \right] (\Gamma\Delta t)^2 \left. \right\} \tag{26}
\end{aligned}$$

Integrating 25 and 26 we obtain:

$$\begin{aligned}
\int R_{odd}(S_\eta, K^{-\pi^+}; \Delta t) e^{-\Gamma|\Delta t|} d(\Delta t) &= \frac{2}{\Gamma} |A_{S_\eta} A_{K^{-\pi^+}}|^2 \left\{ 2 \left(1 + 2\eta\sqrt{R_D} \cos \delta_{K\pi} + R_D \right) \right. \\
&+ \left(\left(1 + \left| \frac{p}{q} \right|^2 \right) + 2\eta\sqrt{R_D} (\cos \delta_{K\pi} + \cos(\delta_{K\pi} - 2\phi)) + R_D \left(1 + \left| \frac{q}{p} \right|^2 \right) \right) y^2 \\
&- \left. \left(\left(1 - \left| \frac{p}{q} \right|^2 \right) + 2\eta\sqrt{R_D} (\cos \delta_{K\pi} - \cos(\delta_{K\pi} - 2\phi)) + R_D \left(1 - \left| \frac{q}{p} \right|^2 \right) \right) x^2 \right\}
\end{aligned} \tag{27}$$

A.5 Double CP tag

For the case of double CP eigenstates (S_+ , S_-) we have:

$$\begin{aligned}
R_{odd}(S_+, S_-; \Delta t) &= |A_{S_+}|^2 |A_{S_-}|^2 \left\{ \left(4 + \left| \frac{p}{q} \right|^2 + \left| \frac{q}{p} \right|^2 + 2 \cos(2\phi) \right) \cosh(y\Gamma\Delta t) \right. \\
&+ \left(4 - \left| \frac{p}{q} \right|^2 - \left| \frac{q}{p} \right|^2 - 2 \cos(2\phi) \right) \cos(x\Gamma\Delta t) \\
&- 4 \cos \phi \left(\left| \frac{q}{p} \right| + \left| \frac{p}{q} \right| \right) \sinh(y\Gamma\Delta t) \\
&+ \left. 4 \sin \phi \left(\left| \frac{q}{p} \right| - \left| \frac{p}{q} \right| \right) \sin(x\Gamma\Delta t) \right\}
\end{aligned} \tag{28}$$

In the limit of $|x\Gamma\Delta t| \ll 1$, $|y\Gamma\Delta t| \ll 1$ we obtain:

$$R_{odd}(S_+, S_-; \Delta t) = |A_{S_+}|^2 |A_{S_-}|^2 \left\{ 2 + \left[\left(\left| \frac{q}{p} \right| - \left| \frac{p}{q} \right| \right) x \sin \phi - \left(\left| \frac{q}{p} \right| + \left| \frac{p}{q} \right| \right) y \cos \phi \right] (\Gamma\Delta t) \right\} \tag{29}$$

It is worth noting that in the above time-dependent rates the charge conjugate expressions can be obtained with the substitutions $|q/p| \leftrightarrow |p/q|$ and $\phi \leftrightarrow -\phi$.

Integrating 28 and 30 we obtain:

$$\begin{aligned}
\int R_{odd}(S_+, S_-; \Delta t) e^{-\Gamma|\Delta t|} d(\Delta t) &= \\
\frac{4}{\Gamma} |A_{S_+}|^2 |A_{S_-}|^2 &\left[4 + \frac{y^2}{2} \left(4 + \left| \frac{p}{q} \right|^2 + \left| \frac{q}{p} \right|^2 + 2 \cos(2\phi) \right) - \frac{x^2}{2} \left(4 - \left| \frac{p}{q} \right|^2 - \left| \frac{q}{p} \right|^2 - 2 \cos(2\phi) \right) \right]
\end{aligned} \tag{30}$$

A.6 Time-dependent Dalitz plot decay rates with CP violation

It is useful to define the Dalitz plot (s_{12}, s_{13}) in terms of kinematical quantities:

$$\begin{aligned} s_{12} &\equiv m_+^2 \equiv m^2(K_S^0 h^+) \\ s_{13} &\equiv m_-^2 \equiv m^2(K_S^0 h^-) \end{aligned} \tag{31}$$

The D^0 decay amplitude varies across the Dalitz plot:

$$\begin{aligned} A_f &\equiv \langle f | \mathcal{H} | D^0 \rangle \equiv A(s_{12}, s_{13}) \equiv A_{s_{12}, s_{13}} \\ \bar{A}_f &\equiv \langle f | \mathcal{H} | \bar{D}^0 \rangle \equiv \bar{A}(s_{12}, s_{13}) \equiv \bar{A}_{s_{12}, s_{13}} \end{aligned} \tag{32}$$

$$\begin{aligned} R_{odd}(S_\eta, K_S^0 h^+ h^-; \Delta t) &= |A_{S_\eta}|^2 \left\{ \right. \\ &\left[|A_f|^2 \left(1 + \left| \frac{p}{q} \right|^2 \right) + |\bar{A}_f|^2 \left(1 + \left| \frac{q}{p} \right|^2 \right) - 4\eta \cos \phi \left(\cos \phi \mathcal{R}e(A_f^* \bar{A}_f) - \sin \phi \mathcal{I}m(A_f^* \bar{A}_f) \right) \right] \cosh(y\Gamma \Delta t) \\ &+ \left[|A_f|^2 \left(1 - \left| \frac{p}{q} \right|^2 \right) + |\bar{A}_f|^2 \left(1 - \left| \frac{q}{p} \right|^2 \right) - 4\eta \sin \phi \left(\sin \phi \mathcal{R}e(A_f^* \bar{A}_f) + \cos \phi \mathcal{I}m(A_f^* \bar{A}_f) \right) \right] \cos(x\Gamma \Delta t) \\ &- 2 \left[\eta \cos \phi \left(\left| \frac{p}{q} \right| |A_f|^2 + \left| \frac{q}{p} \right| |\bar{A}_f|^2 \right) - \left(\left| \frac{q}{p} \right| + \left| \frac{p}{q} \right| \right) \left(\cos \phi \mathcal{R}e(A_f^* \bar{A}_f) - \sin \phi \mathcal{I}m(A_f^* \bar{A}_f) \right) \right] \sinh(y\Gamma \Delta t) \\ &- 2 \left[\eta \sin \phi \left(\left| \frac{p}{q} \right| |A_f|^2 - \left| \frac{q}{p} \right| |\bar{A}_f|^2 \right) - \left(\left| \frac{p}{q} \right| - \left| \frac{q}{p} \right| \right) \left(\sin \phi \mathcal{R}e(A_f^* \bar{A}_f) + \cos \phi \mathcal{I}m(A_f^* \bar{A}_f) \right) \right] \sin(x\Gamma \Delta t) \left. \right\} \end{aligned} \tag{33}$$

In the limit of $|x\Gamma\Delta t| \ll 1$, $|y\Gamma\Delta t| \ll 1$ we obtain:

$$\begin{aligned}
R_{odd}(S_\eta, K_S^0 h^+ h^-; \Delta t) &= |A_{S_\eta}|^2 \left\{ 2 (|A_f|^2 + |\bar{A}_f|^2 - 2\eta \mathcal{R}e(A_f^* \bar{A}_f)) \right. \\
&+ 2 \left[\left(\left| \frac{p}{q} \right| (\cos \phi \mathcal{R}e(A_f^* \bar{A}_f) - \sin \phi \mathcal{I}m(A_f^* \bar{A}_f) - \eta \cos \phi |A_f|^2) \right) + \right. \\
&\quad \left. \left. + \left| \frac{q}{p} \right| (\cos \phi \mathcal{R}e(A_f^* \bar{A}_f) - \sin \phi \mathcal{I}m(A_f^* \bar{A}_f) - \eta \cos \phi |\bar{A}_f|^2) \right) y \right. \\
&- \left(\left| \frac{p}{q} \right| (-\cos \phi \mathcal{I}m(A_f^* \bar{A}_f) - \sin \phi \mathcal{R}e(A_f^* \bar{A}_f) + \eta \sin \phi |A_f|^2) \right) + \\
&\quad \left. \left. + \left| \frac{q}{p} \right| (\cos \phi \mathcal{I}m(A_f^* \bar{A}_f) + \sin \phi \mathcal{R}e(A_f^* \bar{A}_f) - \eta \sin \phi |\bar{A}_f|^2) \right) x \right] (\Gamma \Delta t) \\
&+ \frac{1}{2} \left[\left(|A_f|^2 \left(1 + \left| \frac{p}{q} \right|^2 \right) + |\bar{A}_f|^2 \left(1 + \left| \frac{q}{p} \right|^2 \right) - 4\eta \cos \phi (\cos \phi \mathcal{R}e(A_f^* \bar{A}_f) - \sin \phi \mathcal{I}m(A_f^* \bar{A}_f)) \right) y^2 \right. \\
&- \left. \left(|A_f|^2 \left(1 - \left| \frac{p}{q} \right|^2 \right) + |\bar{A}_f|^2 \left(1 - \left| \frac{q}{p} \right|^2 \right) - 4\eta \sin \phi (\sin \phi \mathcal{R}e(A_f^* \bar{A}_f) + \cos \phi \mathcal{I}m(A_f^* \bar{A}_f)) \right) x^2 \right] (\Gamma \Delta t)^2 \left. \right\} \quad (34)
\end{aligned}$$

Integrating 33 and 34 we obtain:

$$\begin{aligned}
\int R_{odd}(S_\eta, K_S^0 h^+ h^-; \Delta t) e^{-\Gamma|\Delta t|} d(\Delta t) &= \\
&\frac{2}{\Gamma} |A_{S_\eta}|^2 \left\{ 2 (|A_f|^2 + |\bar{A}_f|^2 - 2\eta \mathcal{R}e(A_f^* \bar{A}_f)) \right. \\
&+ \left[\left(|A_f|^2 \left(1 + \left| \frac{p}{q} \right|^2 \right) + |\bar{A}_f|^2 \left(1 + \left| \frac{q}{p} \right|^2 \right) - 4\eta \cos \phi (\cos \phi \mathcal{R}e(A_f^* \bar{A}_f) - \sin \phi \mathcal{I}m(A_f^* \bar{A}_f)) \right) y^2 \right. \\
&- \left. \left(|A_f|^2 \left(1 - \left| \frac{p}{q} \right|^2 \right) + |\bar{A}_f|^2 \left(1 - \left| \frac{q}{p} \right|^2 \right) - 4\eta \sin \phi (\sin \phi \mathcal{R}e(A_f^* \bar{A}_f) + \cos \phi \mathcal{I}m(A_f^* \bar{A}_f)) \right) x^2 \right] \left. \right\} \quad (35)
\end{aligned}$$

that in the limit of CP conservation is:

$$\int R_{odd}(S_\eta, K_S^0 h^+ h^-; \Delta t) e^{-\Gamma|\Delta t|} d(\Delta t) = \frac{4}{\Gamma} |A_{S_\eta}|^2 \left[(|A_f|^2 + |\bar{A}_f|^2 - 2\eta \mathcal{R}e(A_f^* \bar{A}_f)) \right] (1 + y^2) \quad (36)$$

Let's consider now a double Dalitz decay where the final state is identical for the two cases $f_1 = f_2 = K_S^0 h^+ h^-$. The position, (s_{12}, s_{13}) , in the D^0 Dalitz plot for the two final states f_1 and f_2 will be different in general, as well as the respective decay amplitudes:

$$\begin{aligned}
A_{f_1} &\equiv \langle K_S^0 h^+ h^- | \mathcal{H} | D^0 \rangle \equiv A(s_{12}, s_{13}) \equiv A_1 \\
A_{f_2} &\equiv \langle K_S^0 h^+ h^- | \mathcal{H} | D^0 \rangle \equiv A(s'_{12}, s'_{13}) \equiv A_2
\end{aligned} \quad (37)$$

$$\begin{aligned}
R_{odd}(K_S^0 h^+ h^-, K_S^0 h^+ h^-; \Delta t) = & \\
& \left[|\bar{A}_1 A_2|^2 + |A_1 \bar{A}_2|^2 - 2\mathcal{R}e(\bar{A}_1^* A_2^* A_1 \bar{A}_2) \right. \\
& \quad \left. + \left| \frac{p}{q} \right|^2 |A_1 A_2|^2 + \left| \frac{q}{p} \right|^2 |\bar{A}_1 \bar{A}_2|^2 - 2(\cos(2\phi)\mathcal{R}e(A_1^* A_2^* \bar{A}_1 \bar{A}_2) - \sin(2\phi)\mathcal{I}m(A_1^* A_2^* \bar{A}_1 \bar{A}_2)) \right] \cosh(y\Gamma\Delta t) \\
& \left[|\bar{A}_1 A_2|^2 + |A_1 \bar{A}_2|^2 - 2\mathcal{R}e(\bar{A}_1^* A_2^* A_1 \bar{A}_2) \right. \\
& \quad \left. - \left| \frac{p}{q} \right|^2 |A_1 A_2|^2 - \left| \frac{q}{p} \right|^2 |\bar{A}_1 \bar{A}_2|^2 + 2(\cos(2\phi)\mathcal{R}e(A_1^* A_2^* \bar{A}_1 \bar{A}_2) - \sin(2\phi)\mathcal{I}m(A_1^* A_2^* \bar{A}_1 \bar{A}_2)) \right] \cos(x\Gamma\Delta t) \\
& -2 \left[|A_2|^2 \left(\left| \frac{p}{q} \right| (\cos\phi\mathcal{R}e(A_1 \bar{A}_1^*) + \sin\phi\mathcal{I}m(A_1 \bar{A}_1^*) - \mathcal{R}e(A_1 \bar{A}_1^*)) \right) \right. \\
& \quad \left. - |A_1|^2 \left(\left| \frac{p}{q} \right| (\cos\phi\mathcal{R}e(A_2 \bar{A}_2^*) + \sin\phi\mathcal{I}m(A_2 \bar{A}_2^*)) \right) \right. \\
& \quad \left. + |\bar{A}_2|^2 \left(\left| \frac{q}{p} \right| (\cos\phi\mathcal{R}e(\bar{A}_1 A_1^*) - \sin\phi\mathcal{I}m(\bar{A}_1 A_1^*)) \right) \right] \sinh(y\Gamma\Delta t) \\
& +2 \left[|A_2|^2 \left(\left| \frac{p}{q} \right| (\cos\phi\mathcal{I}m(A_1 \bar{A}_1^*) - \sin\phi\mathcal{R}e(A_1 \bar{A}_1^*) - \mathcal{I}m(A_1 \bar{A}_1^*)) \right) \right. \\
& \quad \left. - |A_1|^2 \left(\left| \frac{p}{q} \right| (\cos\phi\mathcal{I}m(A_2 \bar{A}_2^*) - \sin\phi\mathcal{R}e(A_2 \bar{A}_2^*)) \right) \right. \\
& \quad \left. + |\bar{A}_2|^2 \left(\left| \frac{q}{p} \right| (\cos\phi\mathcal{I}m(\bar{A}_1 A_1^*) + \sin\phi\mathcal{R}e(\bar{A}_1 A_1^*)) \right) \right] \sin(x\Gamma\Delta t)
\end{aligned} \tag{38}$$

In the limit of $|x\Gamma\Delta t| \ll 1$, $|y\Gamma\Delta t| \ll 1$ we obtain:

$$\begin{aligned}
& R_{odd}(K_S^0 h^+ h^-, K_S^0 h^+ h^-; \Delta t) = \\
& 2 \left[|\bar{A}_1 A_2|^2 + |A_1 \bar{A}_2|^2 - 2\mathcal{R}e(\bar{A}_1^* A_2^* A_1 \bar{A}_2) \right] \\
& - 2 \left\{ \left[|A_2|^2 \left(\left| \frac{p}{q} \right| (\cos \phi \mathcal{R}e(A_1 \bar{A}_1^*) + \sin \phi \mathcal{I}m(A_1 \bar{A}_1^*) - \mathcal{R}e(A_1 \bar{A}_1^*)) \right) \right. \right. \\
& \quad \left. \left. - |A_1|^2 \left(\left| \frac{p}{q} \right| (\cos \phi \mathcal{R}e(A_2 \bar{A}_2^*) + \sin \phi \mathcal{I}m(A_2 \bar{A}_2^*)) \right) \right. \right. \\
& \quad \left. \left. + |\bar{A}_2|^2 \left(\left| \frac{q}{p} \right| (\cos \phi \mathcal{R}e(\bar{A}_1 A_1^*) - \sin \phi \mathcal{I}m(\bar{A}_1 A_1^*)) \right) \right] y \right. \\
& \quad \left. - \left[|A_2|^2 \left(\left| \frac{p}{q} \right| (\cos \phi \mathcal{I}m(A_1 \bar{A}_1^*) - \sin \phi \mathcal{R}e(A_1 \bar{A}_1^*) - \mathcal{I}m(A_1 \bar{A}_1^*)) \right) \right. \right. \\
& \quad \left. \left. - |A_1|^2 \left(\left| \frac{p}{q} \right| (\cos \phi \mathcal{I}m(A_2 \bar{A}_2^*) - \sin \phi \mathcal{R}e(A_2 \bar{A}_2^*)) \right) \right. \right. \\
& \quad \left. \left. + |\bar{A}_2|^2 \left(\left| \frac{q}{p} \right| (\cos \phi \mathcal{I}m(\bar{A}_1 A_1^*) + \sin \phi \mathcal{R}e(\bar{A}_1 A_1^*)) \right) \right] x \right\} (\Gamma\Delta t) \\
& + \frac{1}{2} \left\{ \left[|\bar{A}_1 A_2|^2 + |A_1 \bar{A}_2|^2 - 2\mathcal{R}e(\bar{A}_1^* A_2^* A_1 \bar{A}_2) \right] (y^2 - x^2) \right. \\
& \quad \left. + \left[\left| \frac{p}{q} \right|^2 |A_1 A_2|^2 + \left| \frac{q}{p} \right|^2 |\bar{A}_1 \bar{A}_2|^2 - 2(\cos(2\phi)\mathcal{R}e(A_1^* A_2^* \bar{A}_1 \bar{A}_2) - \sin(2\phi)\mathcal{I}m(A_1^* A_2^* \bar{A}_1 \bar{A}_2)) \right] (x^2 + y^2) \right\} (\Gamma\Delta t)^2 \\
& \hspace{10cm} (39)
\end{aligned}$$

B D^0 - \bar{D}^0 mixing and CP violation with Dalitz plot analyses

Time-dependent Dalitz plot analyses have been proposed for measuring D^0 - \bar{D}^0 mixing and CPV [5] from CLEO collaboration and extended to a large data sample from BaBar [6], [7] and Belle collaboration [8]. The advantage of performing time-dependent Dalitz plot analyses relies in the possible presence of double Cabibbo suppressed and CP amplitudes, interfering among each other, in a single 3-body decay mode. This characteristic depends on the dynamics of the specific 3-body final state that we are considering.

In addition, for D^0 self-conjugate states (e.g. $K_S^0 h^+ h^-$, $\pi^+ \pi^- \pi^0$) it is possible to extract directly the mixing parameters x , y without D^0 - \bar{D}^0 relative strong phase uncertainties by assuming CP conservation in the D^0 decay. As a drawback, the introduction of a phenomenological model for the parameterization of the 3-body D^0 decay amplitude introduces a “model” uncertainty, sometimes called “Dalitz model” error.

B.1 Considerations for 3-body self-conjugate D^0 decay modes

Self-conjugate 3-body decay modes (e.g. $K_S^0 h^+ h^-$, $\pi^+ \pi^- \pi^0$) have the peculiarity that the final state $|f\rangle$, and the charge conjugate state $C|f\rangle = |\bar{f}\rangle$, can be both identified in a single Dalitz plot (s_{12}, s_{13}) . In particular if $|f\rangle = (s'_{12}, s'_{13})$ then $|\bar{f}\rangle = (s'_{13}, s'_{12})$. For example, this is not possible for the decay mode $D^0 \rightarrow K^+ \pi^- \pi^0$. Time-dependent analysis of self-conjugate 3-body decays with flavor tag allows to extract mixing parameters x , y directly when assuming CP conservation in the decay amplitude, $\bar{A}_f \equiv A_{\bar{f}}$. Infact the time-dependence:

$$\begin{aligned} \frac{d\Gamma[D_{\text{phys}}^0 \rightarrow f]/dt}{e^{-\Gamma t} \mathcal{N}_f} &= \left[(|A_f|^2 + |\frac{q}{p}|^2 |\bar{A}_f|^2) \cosh(\Gamma y t) + (|A_f|^2 - |\frac{q}{p}|^2 |\bar{A}_f|^2) \cos(\Gamma x t) \right. \\ &\quad \left. + 2\mathcal{R}e \left(A_f^* \bar{A}_f \frac{q}{p} \right) \sinh(\Gamma y t) - 2\mathcal{I}m \left(A_f^* \bar{A}_f \frac{q}{p} \right) \sin(\Gamma x t) \right] \end{aligned} \quad (40)$$

with CP assumed to be conserved in the decay becomes:

$$\begin{aligned} \frac{d\Gamma[D_{\text{phys}}^0 \rightarrow f]/dt}{e^{-\Gamma t} \mathcal{N}_f} &= \left[(|A_f|^2 + |\frac{q}{p}|^2 |A_{\bar{f}}|^2) \cosh(\Gamma y t) + (|A_f|^2 - |\frac{q}{p}|^2 |A_{\bar{f}}|^2) \cos(\Gamma x t) \right. \\ &\quad \left. + 2\mathcal{R}e \left(A_f^* A_{\bar{f}} \frac{q}{p} \right) \sinh(\Gamma y t) - 2\mathcal{I}m \left(A_f^* A_{\bar{f}} \frac{q}{p} \right) \sin(\Gamma x t) \right] \end{aligned} \quad (41)$$

which is written in terms of the D^0 decay amplitude and can be fitted directly from the data. In Eq. 41 is no more present the \bar{D}^0 decay amplitude or the relative D^0 - \bar{D}^0 strong phase.

In general CP is conserved in the decay of charm meson with a good precision in the Standard Model. However, for D^0 decays with a K_S^0 final particle, CP violation is expected to be observed at the level of 0.3% due to CPV in the $K^0 - \bar{K}^0$ mixing. This effect is probably not negligible for the level of precision that we want to achieve at SuperB (*need to be more quantitative on this point*). In addition the Dalitz model error will probably limit the precision of these measurements when the high statistics data sample will be available.

B.2 Relevance of D^0 - \bar{D}^0 threshold data

Measurements at D^0 - \bar{D}^0 threshold will definitely help in reducing the Dalitz model uncertainty and also in avoiding the need of the assumption of CP conservation in the D^0 decay. Let's consider for the moment the time-integrated rate, reported in Eq. 35. For each Dalitz plot region or bin, identified with the index i , we have the possibility to access the information on the relative D^0 - \bar{D}^0 phase as reported below:

$$\begin{aligned} & \int_i d\mathcal{P} \int d(\Delta t) \left[\frac{R_{\text{odd}}(S_-, K_S^0 h^+ h^-; \Delta t)}{|A_{S_-}|^2} - \frac{R_{\text{odd}}(S_+, K_S^0 h^+ h^-; \Delta t)}{|A_{S_+}|^2} \right] e^{-\Gamma|\Delta t|} = \\ & \frac{16}{\Gamma} \int_i d\mathcal{P} \left[\mathcal{R}e(A_f^* \bar{A}_f) (1 + y^2 \cos^2 \phi - x^2 \sin^2 \phi) - \mathcal{I}m(A_f^* \bar{A}_f) \cos \phi \sin \phi (x^2 + y^2) \right] = \\ & \frac{16}{\Gamma} \int_i d\mathcal{P} [\mathcal{R}e(A_f^* \bar{A}_f) + \mathcal{O}(x^2 + y^2)] = \frac{16}{\Gamma} c_i \sqrt{T_i \bar{T}_i} + \mathcal{O}(x^2 + y^2) \end{aligned} \quad (42)$$

$$\begin{aligned} \int_i d\mathcal{P} \int dt \frac{d\Gamma[D_{\text{phys}}^0 \rightarrow f]/dt}{2\mathcal{N}_f/\Gamma} &= \frac{1}{2} \int_i d\mathcal{P} \left[(|A_f|^2 + |\frac{q}{p}|^2 |\bar{A}_f|^2) \frac{1}{1-y^2} + (|A_f|^2 - |\frac{q}{p}|^2 |\bar{A}_f|^2) \frac{1}{1+x^2} \right] \\ &\simeq \frac{1}{2} \int_i d\mathcal{P} \left[(2 + y^2 - x^2) |A_f|^2 + \left(|\frac{q}{p}|^2 |\bar{A}_f|^2 \right) (x^2 + y^2) \right] = \\ & T_i \left(1 + \frac{y^2 - x^2}{2} \right) + \bar{T}_i \left(\left| \frac{q}{p} \right|^2 \frac{x^2 + y^2}{2} \right) \end{aligned} \quad (43)$$

$$\begin{aligned} \int_i d\mathcal{P} \int dt \frac{d\Gamma[\bar{D}_{\text{phys}}^0 \rightarrow f]/dt}{2\mathcal{N}_f/\Gamma} &= \frac{1}{2} \int_i d\mathcal{P} \left[(|\bar{A}_f|^2 + |\frac{p}{q}|^2 |A_f|^2) \frac{1}{1-y^2} + (|\bar{A}_f|^2 - |\frac{p}{q}|^2 |A_f|^2) \frac{1}{1+x^2} \right] \\ &\simeq \frac{1}{2} \int_i d\mathcal{P} \left[(2 + y^2 - x^2) |\bar{A}_f|^2 + \left(|\frac{p}{q}|^2 |A_f|^2 \right) (x^2 + y^2) \right] = \\ & \bar{T}_i \left(1 + \frac{y^2 - x^2}{2} \right) + T_i \left(\left| \frac{p}{q} \right|^2 \frac{x^2 + y^2}{2} \right) \end{aligned} \quad (44)$$

where $\int_i d\mathcal{P}$ indicates the integral over the phase space relative to the Dalitz plot bin i and also

$$\begin{aligned} A_f &= |A_f| e^{i\delta_f} & \bar{A}_f &= |\bar{A}_f| e^{i\bar{\delta}_f} \\ \int_i |A_f|^2 d\mathcal{P} &= T_i & \int_i |\bar{A}_f|^2 d\mathcal{P} &= \bar{T}_i \\ \frac{\int_i \mathcal{R}e(A_f^* \bar{A}_f) d\mathcal{P}}{\sqrt{T_i \bar{T}_i}} &= \frac{\int_i |A_f| |\bar{A}_f| \cos(\bar{\delta}_f - \delta_f) d\mathcal{P}}{\sqrt{T_i \bar{T}_i}} = c_i \\ \frac{\int_i \mathcal{I}m(A_f^* \bar{A}_f) d\mathcal{P}}{\sqrt{T_i \bar{T}_i}} &= \frac{\int_i |A_f| |\bar{A}_f| \sin(\bar{\delta}_f - \delta_f) d\mathcal{P}}{\sqrt{T_i \bar{T}_i}} = s_i \end{aligned} \quad (45)$$

For 3-body self-conjugate decay modes the relations $c_i \equiv c_{\bar{i}}$ and $s_i \equiv -s_{\bar{i}}$ hold in case of CP conservation in the decay. Here, with \bar{i} we intend the Dalitz plot region or bin obtained by mirroring the bin i over the axis of symmetry of the Dalitz plot. In case bin sizes are chosen in such a way that the amplitude variation within the i -th bin is relatively small, the following approximation might be used to determine the s_i coefficients $|s_i| = \sqrt{1 - c_i^2}$ and the s_i sign could be determined directly from the data as proposed by Bondar *et al.* [9; 10]. In particular in [9] it is shown how the double-tag $(K_S^0 \pi^+ \pi^-)_D (K_S^0 \pi^+ \pi^-)_D$ events improve the determination of s_i .

Eq. 40 can be written in a model independent way for each bin i of the Dalitz plot in terms of the coefficient c_i, s_i, T_i, \bar{T}_i :

$$\begin{aligned} \frac{d\Gamma_i[D_{\text{phys}}^0 \rightarrow f]/dt}{e^{-\Gamma t} \mathcal{N}_f} &= \left[\left(T_i + \left| \frac{q}{p} \right|^2 \bar{T}_i \right) \cosh(\Gamma y t) + \left(T_i - \left| \frac{q}{p} \right|^2 \bar{T}_i \right) \cos(\Gamma x t) \right. \\ &+ 2 \left(c_i \sqrt{T_i \bar{T}_i} \left| \frac{q}{p} \right| \cos \phi - s_i \sqrt{T_i \bar{T}_i} \left| \frac{q}{p} \right| \sin \phi \right) \sinh(\Gamma y t) \\ &\left. - 2 \left(c_i \sqrt{T_i \bar{T}_i} \left| \frac{q}{p} \right| \sin \phi + s_i \sqrt{T_i \bar{T}_i} \left| \frac{q}{p} \right| \cos \phi \right) \sin(\Gamma x t) \right] \end{aligned} \quad (46)$$

The above time-dependence does not assume CP conservation in the decay of the D^0 and also does not require any phenomenological parameterization of the D^0 decay amplitude. The parameters c_i, s_i can be obtained in a time-integrated measurement of $(K_S^0 \pi^+ \pi^-)_D$ decays at D^0 - \bar{D}^0 threshold as explained above, and the parameters T_i, \bar{T}_i can be extracted with a time-integrated measurement of flavor tagged decays both at the $\Upsilon(4S)$ and at D^0 - \bar{D}^0 threshold. In both cases, the relative uncertainty on the extraction of the parameters from the time-integrated measurements is about $10^{-4} \simeq \mathcal{O}(x^2 + y^2)$ or lower.

We report here eq. 6 again for convenience:

$$\begin{aligned} \frac{d\Gamma[V_{\text{phys}}(t_1, t_2) \rightarrow f_1 f_2]/dt}{e^{-\Gamma|\Delta t|}\mathcal{N}_{f_1 f_2}} = \\ (|a_+|^2 + |a_-|^2) \cosh(y\Gamma\Delta t) + (|a_+|^2 - |a_-|^2) \cos(x\Gamma\Delta t) \\ - 2\mathcal{R}e((a_+^* a_-) \sinh(y\Gamma\Delta t) + 2\mathcal{I}m(a_+^* a_-) \sin(x\Gamma\Delta t)) \end{aligned} \quad (47)$$

From the definition of a_+ and a_- it follows:

$$|a_+|^2 = |\bar{A}_{f_1}|^2 |A_{f_2}|^2 + |A_{f_1}|^2 |\bar{A}_{f_2}|^2 - 2\mathcal{R}e(\bar{A}_{f_1} A_{f_2} A_{f_1}^* \bar{A}_{f_2}^*) \quad (48)$$

$$|a_-|^2 = |p/q|^2 |A_{f_1}|^2 |A_{f_2}|^2 + |q/p|^2 |\bar{A}_{f_1}|^2 |\bar{A}_{f_2}|^2 - 2\mathcal{R}e(p/q p^*/q^* A_{f_1} \bar{A}_{f_1}^* A_{f_2} \bar{A}_{f_2}^*) \quad (49)$$

$$a_+^* a_- = p/q |A_{f_2}|^2 A_{f_1} \bar{A}_{f_1}^* - p/q |A_{f_1}|^2 A_{f_2} \bar{A}_{f_2}^* - q/p |\bar{A}_{f_1}|^2 A_{f_2}^* \bar{A}_{f_2} + q/p |\bar{A}_{f_2}|^2 A_{f_1}^* \bar{A}_{f_1} \quad (50)$$

We define:

$$\int_i |A_{f_j}|^2 dP = T_{ji} \quad (51)$$

$$\int_i |\bar{A}_{f_j}|^2 dP = \bar{T}_{ji} \quad (52)$$

$$\int_i \bar{A}_{f_j}^* A_{f_j} dP = \sqrt{T_{ji} \bar{T}_{ji}} (c_{ji} + i s_{ji}) \quad (53)$$

where $\int_i dP$ is the integral over the i -th bin of the Dalitz plot, $j = 1, 2$ indicates the two D decays and c_{ji} and s_{ji} are the real and imaginary part of $\int_i dP / \sqrt{T_{ji} \bar{T}_{ji}}$, respectively.

$$\int_i \int_j |a_+|^2 = \bar{T}_{1i} T_{2j} + T_{1i} \bar{T}_{2j} - 2\sqrt{T_{1i} \bar{T}_{1i} T_{2j} \bar{T}_{2j}} (c_{1i} c_{2j} + s_{1i} s_{2j}) \quad (54)$$

$$\begin{aligned} \int_i \int_j |a_-|^2 = & \left| \frac{p}{q} \right|^2 T_{1i} T_{2j} + \left| \frac{q}{p} \right|^2 \bar{T}_{1i} \bar{T}_{2j} - \\ & 2\sqrt{T_{1i} \bar{T}_{1i} T_{2j} \bar{T}_{2j}} (\cos 2\phi (c_{1i} c_{2j} - s_{1i} s_{2j}) - \sin 2\phi (c_{1i} s_{2j} + s_{1i} c_{2j})) \end{aligned} \quad (55)$$

$$\begin{aligned} \int_i \int_j \mathcal{R}e(a_+^* a_-) = & \left(\left| \frac{p}{q} \right| T_{2j} + \left| \frac{q}{p} \right| \bar{T}_{2j} \right) \sqrt{T_{1i} \bar{T}_{1i}} (\cos \phi c_{1i} + \sin \phi s_{1i}) - \\ & \left(\left| \frac{p}{q} \right| T_{1i} + \left| \frac{q}{p} \right| \bar{T}_{1i} \right) \sqrt{T_{2j} \bar{T}_{2j}} (\cos \phi c_{2j} + \sin \phi s_{2j}) \end{aligned} \quad (56)$$

$$\begin{aligned} \int_i \int_j \mathcal{I}m(a_+^* a_-) = & \left(\left| \frac{p}{q} \right| T_{2j} + \left| \frac{q}{p} \right| \bar{T}_{2j} \right) \sqrt{T_{1i} \bar{T}_{1i}} (\cos \phi s_{1i} - \sin \phi c_{1i}) - \\ & \left(\left| \frac{p}{q} \right| T_{1i} + \left| \frac{q}{p} \right| \bar{T}_{1i} \right) \sqrt{T_{2j} \bar{T}_{2j}} (\cos \phi s_{2j} - \sin \phi c_{2j}); \end{aligned} \quad (57)$$

Relations 54-57 put in 47 tells what can be gained by performing a double- $K_S^0 \pi^+ \pi^-$ time-dependent analysis compared to the time-integrated case, where one is basically sensitive to the $|a_+|^2$ term only.